Applied Innovations in Industrial Robotics: Increasing Operational Range through Structural Modifications and Control System Analysis

MSc. Orges BESHKU[1]
IV-Automation Management Consulting sh.p.k

Abstract

This article focuses on the studying and improving of the capabilities of a Fanuc M-900iB, 6 degree of freedom industrial robot arm. The main objective is to increase its reach and expand its workspace in situations where parallel production lines in automated industries can use one robot with a wide work frame instead of two robots per each line. In order to achieve these objectives, a complete engineering study of the structural, mechanical, electrical, electronic and software components has been carried out. To make this analysis, evaluation and improvement, the maintenance and construction manuals of this robot, the computer program used in real life as well as its physical study and computer simulation were used as reference.

[1] Orges Beshku is a highly accomplished automation expert and technology innovator, with expertise in automation, robotics, and marine electronics. He is the Founder & CEO of IVy Ltd., where he leads digital transformation and automation management consulting projects across various industries, specializing in advanced technologies like IoT and Industry 4.0. Orges is also a Lecturer of Robotics & Electronics at the European University of Tirana, where he contributes to both teaching and research in the field. Currently serving as Head of Engineering at Durrës Port Authority Inc., Orges oversees major engineering initiatives, including the modernization of port infrastructure and machinery. Orges holds a Master of Science in Mechatronics Engineering from the Polytechnic University of Tirana, where his research focused on improving industrial robotic systems. He is certified in multiple technical and management fields, including PLC programming, advanced robotics, marine electronics, port management, and leadership in times of change.

In the mechanical aspect, the structure is studied with all the constituent components such as the base, the joints, the end effector and the links between them with the weight of each component, electrical consumption, ranges of motion, angular velocities, moments of inertia as well as internal components have been considered while the second part of the mechanics covers the kinematics and dynamics in mathematical aspects and computer simulations of the trajectory of its movement, considering the inertia created in the minimum and maximum capacity.

In the electrical/electronic aspect, the configuration has been studied in detail including the control unit, main board, servo amplifier, servo motors, power supply unit and transformer. In the second part, the electronic control method, general control block diagrams as well as specific position, speed, and current control block diagrams are presented, explaining the filters and amplifiers associated with each, Bode diagrams, and characteristics of open and closed systems. In conclusion links 1 and 3 were extended by 0.3m and 0.25m, offering us a much wider and effective working frame of the robot in the workplace. According to the simulations performed the forces required by the change are affordable and within the safety factor for the supply unit with power, amplifier and servo motors.

Keywords: *Industrial Robotics, Control System Analysis, Structural Modification, Automated Industries, Structural & System Integrity, Kinematics & Dynamics*

1. The robotic system

The field of robotics has progressed rapidly over the past few decades, with an increasing number of robots being used in various industrial and commercial applications. One of the most popular and versatile robots used in industry today is the FANUC M-900iB. This is an industrial robot designed for applications that require high speed and load capacity with a maximum capacity of 360 kg and a reach of 2655 mm. The six-angle-of-freedom configuration of the robot allows for a wide range of motion and flexibility in a variety of applications.

In this research article, the dynamics and control of the FANUC M-900iB/360 robot, the various factors that contribute to the robot's performance, including its mechanical structure, actuation system and control algorithms, will be examined in detail. By analysing these factors, we aim to gain a deeper understanding of robot behaviour and dynamic control and provide insights that can lead to further improvements in the performance and capabilities of this important industrial tool.

FIGURE 1 – Mechanical Structure

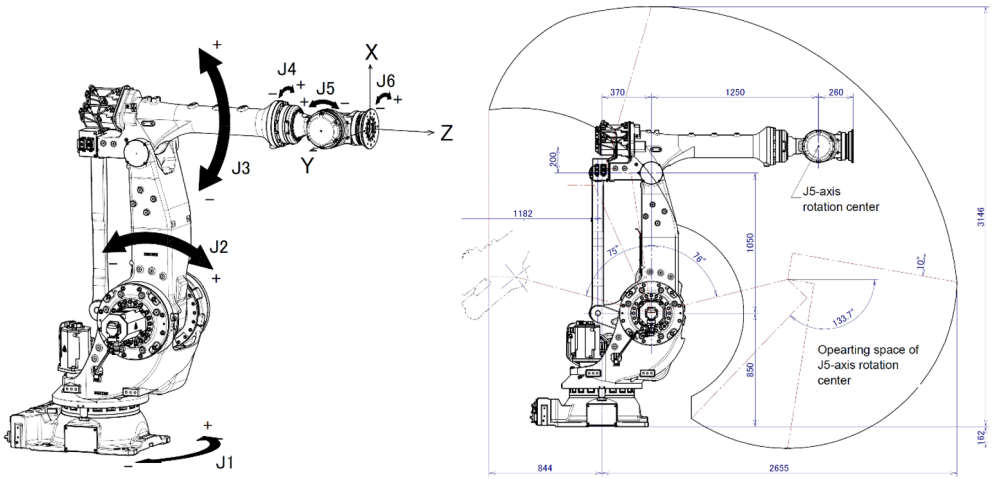

1.1 AI Generated scenarios

Two parallel production lines with two Fanuc robots:
In this scenario, a factory operates two parallel production lines, each producing boxes of varying sizes and colours. Two Fanuc robots, one positioned beside each production line, are tasked with palletizing the boxes onto adjacent pallets.

One central robot with elongated arms handling two production lines:
In this scenario, a single Fanuc robot, centrally located between two parallel production lines, is responsible for palletizing the output from both lines. The robot has elongated arms, allowing it to reach the boxes coming from both lines. This setup reduces the need for multiple robots, optimizing space and operational costs while maintaining efficiency.

FIGURE 2 – Standard M900-iB robotic arms working on 2 production lines

FIGURE 3 – Single modified M900-iB robotic arm working on 2 production lines

2. Methodology

The robot manufacturer's own manuals, descriptions, specifications and methods will be used to analyse and evaluate the robotic system in accordance with the robot's function. The analysis will be done to work as a robotic palletizing arm and will be compared with the real work values of the robot to prove the accuracy of the simulation. Also, mathematical models assisted by simulations in software like Matlab, RoboAnalyzer will be used to evaluate the capabilities of the current system and conclude if this system is able to withstand structural changes based on the changes made.

3. Mechanics

3.1 Mechanical Structure

The mechanical structure of the FANUC M-900iB/360 robot consists of several key components, including the base, six joints (J1-J6), links, and end effector.

The base of the robot is usually mounted on a pedestal or a floor fixture and provides a stable base for the rest of the robot. The six robot joints (J1-J6) are responsible for providing the robot with six degrees of freedom, allowing it to move in different directions and orientations. The end effector of the robot is responsible for performing specific tasks, such as grasping or manipulating objects.

Overall, the mechanical structure of the FANUC M-900iB/360 robot is designed to provide maximum flexibility and manoeuvrability while maintaining stability and precision during operation.

FIGURE 4 – Degrees of freedom and their limits

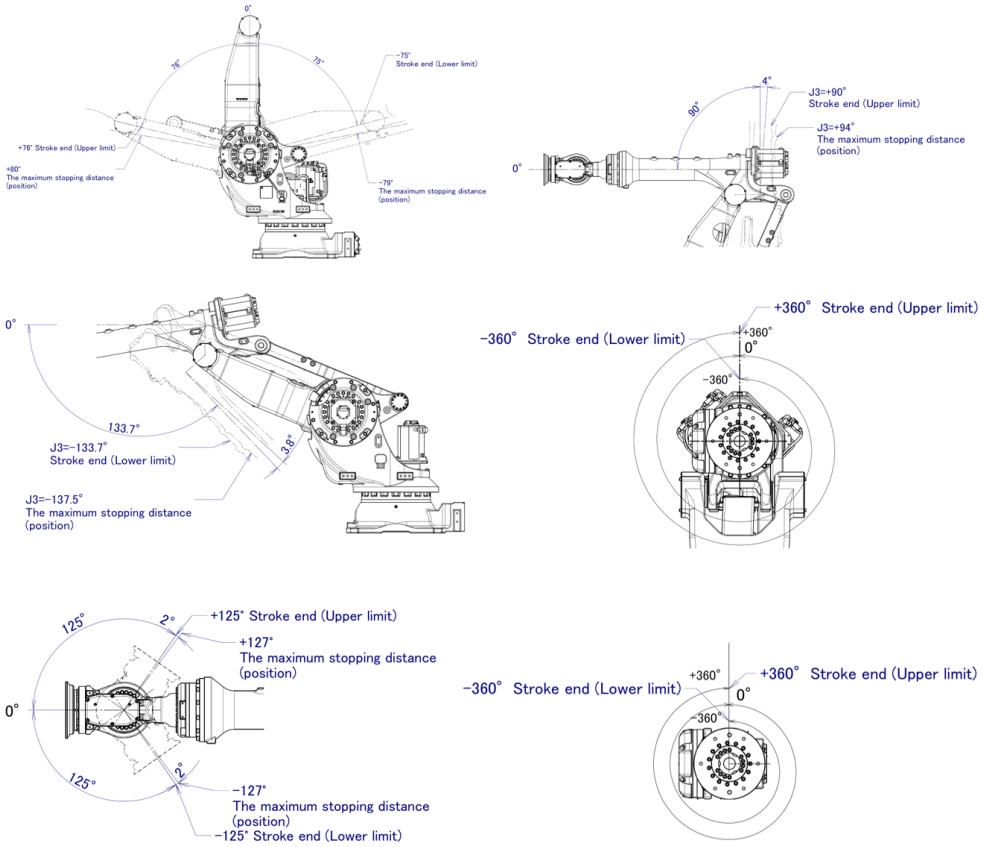

3.2 Kinematics

Forward kinematics is the study of the manipulator to find the position and orientation of the tip or end effector using the joint values of the manipulator. The first step of performing forward kinematics is determining the lengths of the links, the second step is setting the frames and finally, through the obtained matrices, we find the final homogeneous matrix.

FIGURE 5 - FANUC M-900iB simulated on RoboAnalyzer

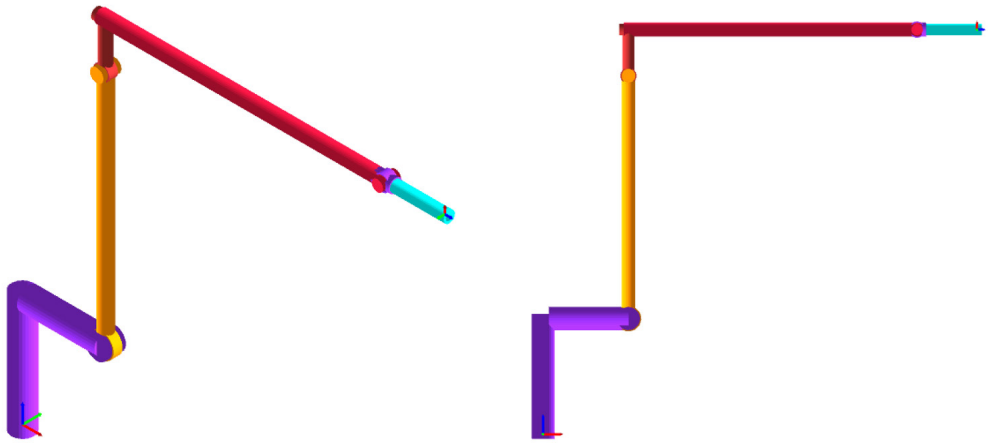

D-H parameters can be found based on frame assignment. These parameters are illustrated in table 4:

FIGURE 6 - D-H Parameters

Link no.	Link type	Link length d (z) (m)	θ (°)	Link displacement a (x) (m)	α (°)	Initial angle	Final angle
1	R	0.5	Var	0.37	90	0	Θ1
2	R	0	Var	1.05	0	0	Θ2
3	R	0	Var	0.2	90	0	Θ3
4	R	1.25	Var	0	90	0	Θ4
5	R	0	Var	0	-90	0	Θ5
6	R	0.26	Var	0	0	0	Θ6

The transformation matrix for a link i is described as follows:

$$A_i = \begin{bmatrix} \cos\theta i & -\sin\theta i \cos\alpha i & \sin\theta i \sin\alpha i & \alpha i \cos\theta i \\ \sin\theta i & \cos\theta i \cos\alpha i & -\cos\theta i \sin\alpha i & \alpha i \sin\theta i \\ 0 & \sin\alpha i & \cos\alpha i & \mathrm{d}i \\ 0 & 0 & 0 & 1 \end{bmatrix}$$

And the resulting matrices for each link are:

$$T_1^0 = \begin{bmatrix} \cos\theta1 & 0 & \sin\theta1 & 0.37\cos\theta1 \\ \sin\theta1 & 0 & -\cos\theta1 & 0.37\sin\theta1 \\ 0 & 1 & 0 & 0.5 \\ 0 & 0 & 0 & 1 \end{bmatrix}, \quad T_2^1 = \begin{bmatrix} \cos\theta2 & -\sin\theta2 & 0 & 1.05\cos\theta2 \\ \sin\theta2 & \cos\theta2 & 0 & 1.05\sin\theta2 \\ 0 & 0 & 1 & 0 \\ 0 & 0 & 0 & 1 \end{bmatrix}, \quad T_3^2 = \begin{bmatrix} \cos\theta3 & 0 & \sin\theta3 & 0.2\cos\theta3 \\ \sin\theta3 & 0 & -\cos\theta3 & 0.2\sin\theta3 \\ 0 & 1 & 0 & 0 \\ 0 & 0 & 0 & 1 \end{bmatrix}$$

$$T_4^3 = \begin{bmatrix} \cos\theta4 & 0 & -\sin\theta4 & 0 \\ \sin\theta4 & 0 & \cos\theta4 & 0 \\ 0 & -1 & 0 & 1.25 \\ 0 & 0 & 0 & 1 \end{bmatrix}, \quad T_5^4 = \begin{bmatrix} \cos\theta5 & 0 & \sin\theta5 & 0 \\ \sin\theta5 & 0 & -\cos\theta5 & 0 \\ 0 & 1 & 0 & 0 \\ 0 & 0 & 0 & 1 \end{bmatrix}, \quad T_6^5 = \begin{bmatrix} \cos\theta6 & -\sin\theta6 & 0 & 0 \\ \sin\theta6 & \cos\theta6 & 0 & 0 \\ 0 & 0 & 1 & 0.26 \\ 0 & 0 & 0 & 1 \end{bmatrix}$$

In the base position of the robot where all the initial angles are 0°, we determine the positions and rotations between the base and the links as well as between the preceding links. The resulting matrices are:

$$\boldsymbol{T_0^1} = \begin{pmatrix} 1 & 0 & 0 & 0.37 \\ 0 & 0 & -1 & 0 \\ 0 & 1 & 0 & 0.5 \\ 0 & 0 & 0 & 1 \end{pmatrix} \boldsymbol{T_1^2} = \begin{pmatrix} 0 & 1 & 0 & 0 \\ 1 & 0 & 0 & 1.05 \\ 0 & 0 & -1 & 0 \\ 0 & 0 & 0 & 1 \end{pmatrix} \boldsymbol{T_2^3} = \begin{pmatrix} 1 & 0 & 0 & 0.2 \\ 0 & 0 & 1 & 0 \\ 0 & -1 & 0 & 0 \\ 0 & 0 & 0 & 1 \end{pmatrix}$$

$$\boldsymbol{T_3^4} = \begin{pmatrix} 1 & 0 & 0 & 0 \\ 0 & 0 & 1 & 0 \\ 0 & -1 & 0 & 1.25 \\ 0 & 0 & 0 & 1 \end{pmatrix} \boldsymbol{T_4^5} = \begin{pmatrix} 1 & 0 & 0 & 0 \\ 0 & 0 & 1 & 0 \\ 0 & -1 & 0 & 0 \\ 0 & 0 & 0 & 1 \end{pmatrix} \boldsymbol{T_5^6} = \begin{pmatrix} 1 & 0 & 0 & 0 \\ 0 & 1 & 0 & 0 \\ 0 & 0 & 1 & 0.26 \\ 0 & 0 & 0 & 1 \end{pmatrix}$$

The resulting matrix gained from matrix multiplication shows the final rotation and position of the end effector of the robot.

$$T_6^0 = T_1^0 \times T_2^1 \times T_3^2 \times T_4^3 \times T_5^4 \times T_6^5,$$

$$T_6^0 = \begin{bmatrix} r11 & r12 & r13 & Px \\ r21 & r22 & r23 & Py \\ r31 & r32 & r33 & Pz \\ 0 & 0 & 0 & 1 \end{bmatrix},$$

$$T_6^0 = \begin{bmatrix} R_6^0 & P_6^0 \\ 0 & 1 \end{bmatrix}.$$

$$\boldsymbol{T_0^6} = \begin{pmatrix} 1 & 0 & 0 & 1.88 \\ 0 & -1 & 0 & 0 \\ 0 & 0 & 1 & 1.75 \\ 0 & 0 & 0 & 1 \end{pmatrix}$$

3.3 Computer simulation of dynamics

Robot dynamics is a subfield of robotics that deals with the study of the motion and forces of robots. It focuses on understanding the relationships between the motion of a robot, the forces that cause that motion, and the physical properties of the robot itself, and is important for their design and control. It is used to analyse the performance of these systems, including speed, accuracy and stability of movements.

To model and analyse the dynamics of the robot, mathematical models are used, such as the equations of motion, which describe the movement of the robot under the influence of forces. These models take into account the kinematics (position, velocity and acceleration) of the robot, as well as the forces and torques acting on it, but it is possible to simulate their dynamics in software and that is how the robot is. studied in this project. By calculating the dimensions, weight and moments of inertia of each link, a computer model identical to the physical one was designed to which a maximum load was applied to the end effector and its behaviour in movement with a complex trajectory was analysed.

This simulation not only gives us details of the movement of the robot with the data set by us, but also correctly shows the outer limits and the working range of the robot which coincides with that presented in the technical documents of the manufacturing company, which proves the accuracy of simulation.

As seen in figure 5 and 6, there are 2 tables where the first one contains the parameters of the original robot and the second one contains the parameters of the proposed robot, where what is noticed is the addition of 0.3m (from 0.5m to 0.8m) in the link first as well as for the third link with 0.25m (from 1.25m to 1.5m). Based on these values, the simulation and comparison between the systems will be done.

FIGURE 7 - D-H Parameters during simulation for original lengths

Link no.	Link type	Link length d (z) (m)	θ (°)	Link displacement a (x) (m)	α (°)	Initial angle	Final angle
1	R	0.5	Var	0.37	90	0	3600
2	R	0	Var	1.05	0	14	90
3	R	0	Var	0.2	90	-70	90
4	R	1.25	Var	0	90	0	720
5	R	0	Var	0	-90	125	-125
6	R	0.26	Var	0	0	0	720

FIGURE 8 - D-H Parameters during simulation for modified lengths

Link no.	Link type	Link length d (z) (m)	θ (°)	Link displacement a (x) (m)	α (°)	Initial angle	Final angle
1	R	0.8	Var	0.37	90	0	3600
2	R	0	Var	1.05	0	14	90
3	R	0	Var	0.2	90	-70	90
4	R	1.5	Var	0	90	0	720
5	R	0	Var	0	-90	125	-125
6	R	0.26	Var	0	0	0	720

FIGURE 9 - Simulated working range and frame before and after modifications.

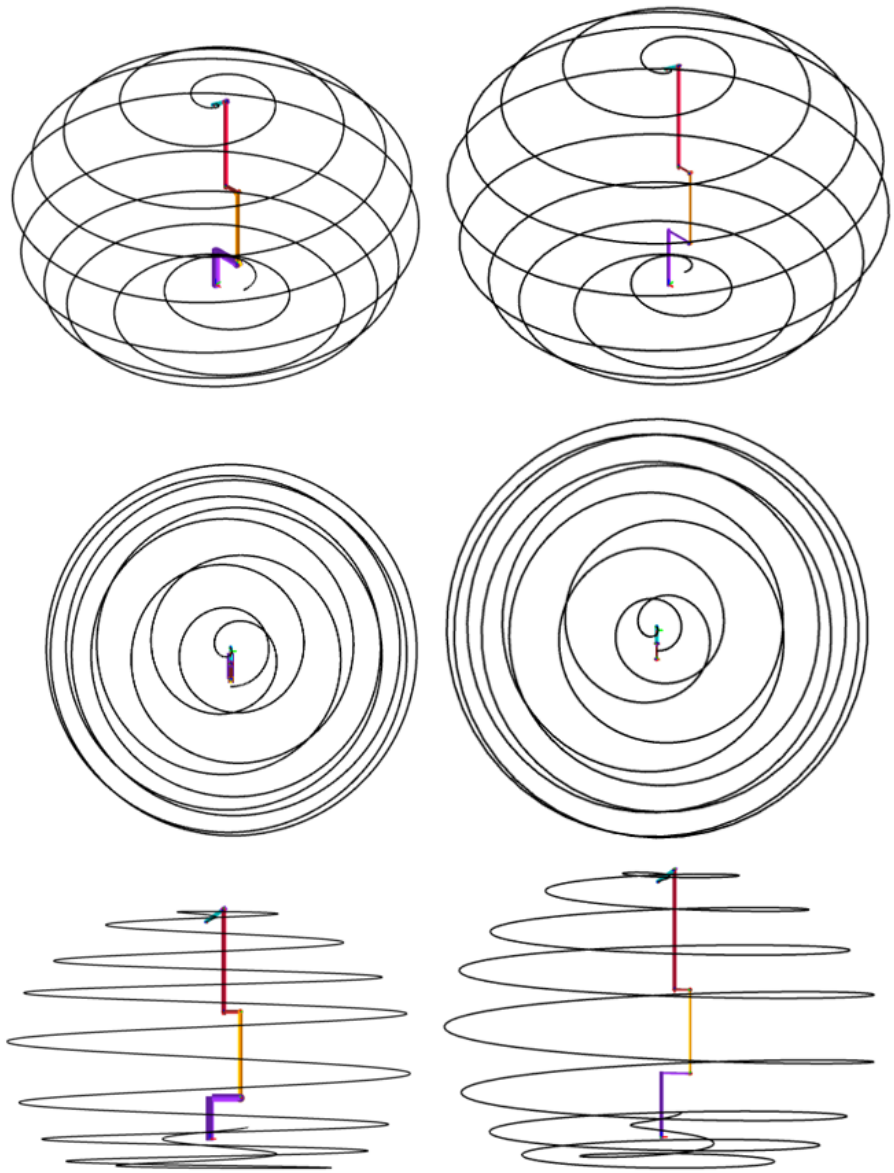

As can be seen in Figure 7, the working frame range of the proposed robot is significantly larger than the working frame range of the existing robot. This is a positive result in the first simulations, but it should be taken into account that the extension of the links leads to an increase in the moment of rotation of the arm, bringing the need for more force. If the required force is within the parameters of the existing servo motors, then no other changes are needed to improve this system structurally.

The values recorded in the program to correctly determine the forces are:

Link	Mass (kg)	Inertia I_{xx} (kgm^2)	Inertia I_{yy} (kgm^2)	Inertia I_{zz} (kgm^2)
1	350	16.6	23.26	25.28
2	280	27.85	4.2	27.85
3	240	21.8	21.25	3.05
4	60	0.76	0.76	0.6
5	20	0.26	0.21	0.25
6	20 + 360	0.1	0.1	0.1

In the created simulation, the geometric movements, speeds, accelerations and forces needed to perform the movements of the robot in the defined trajectory were measured. Each of the measurements is made at the endpoint of the link and each link is dependent on the previous one. The physical parameters are defined in the table above.

The starting point is set as figure 8 to ensure that during rotations we also get the maximum working range of the robot. Also in this figure is the simulation of the starting position with the proposed changes to the body of the robot.

FIGURE 10 - Simulation of starting point position

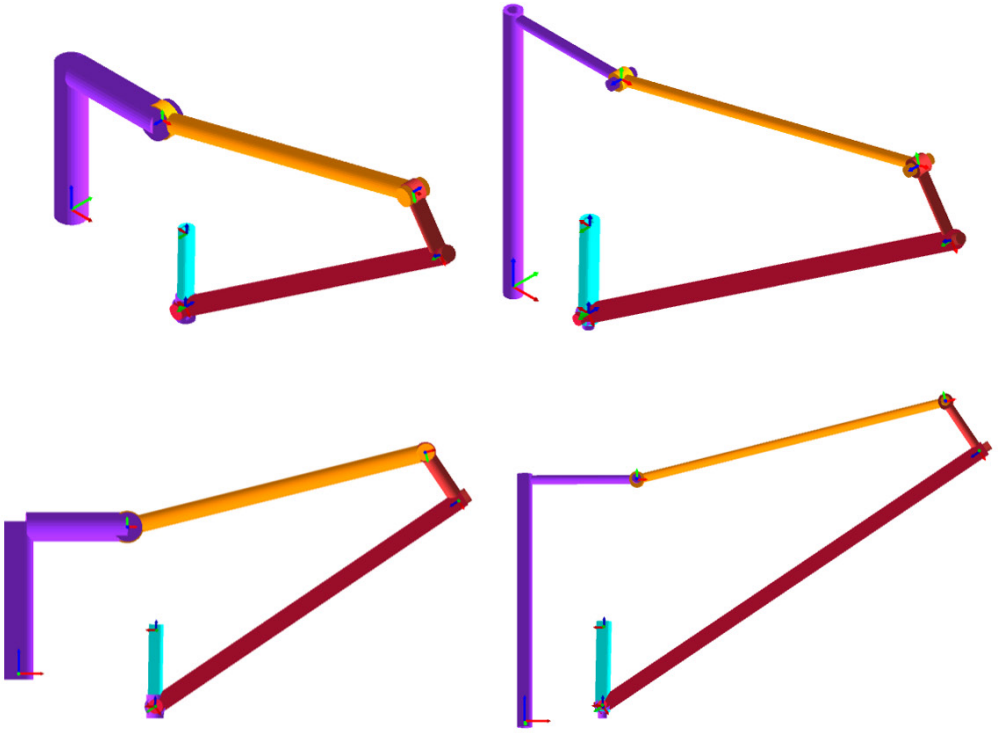

In the summary graph (figure 9) we see and compare more clearly the trends of all links and their maximum values. What interests us and proves the accuracy of the geometric simulation is the maximum position of link 6 in the y and z axis. According to the specifications of the robot from the manufacturing company, the maximum values of y and z are 2655mm and 3160mm respectively, but in z the base of 350mm is also taken into account, which is not taken into account in the simulation of our robot. This makes the z of this a value of 2810mm.

The simulation shows that the maximum values of y and z of link 6 are 2655mm and 2810mm, respectively, which proves the accuracy of the simulation from the geometric point of view. While in the new proposed system we have a maximum z height of 3360mm and a maximum width of 2900mm, in contrast to the manufacturer's 2655.

FIGURE 11 - Simulation of the position of 6 links before and after modification

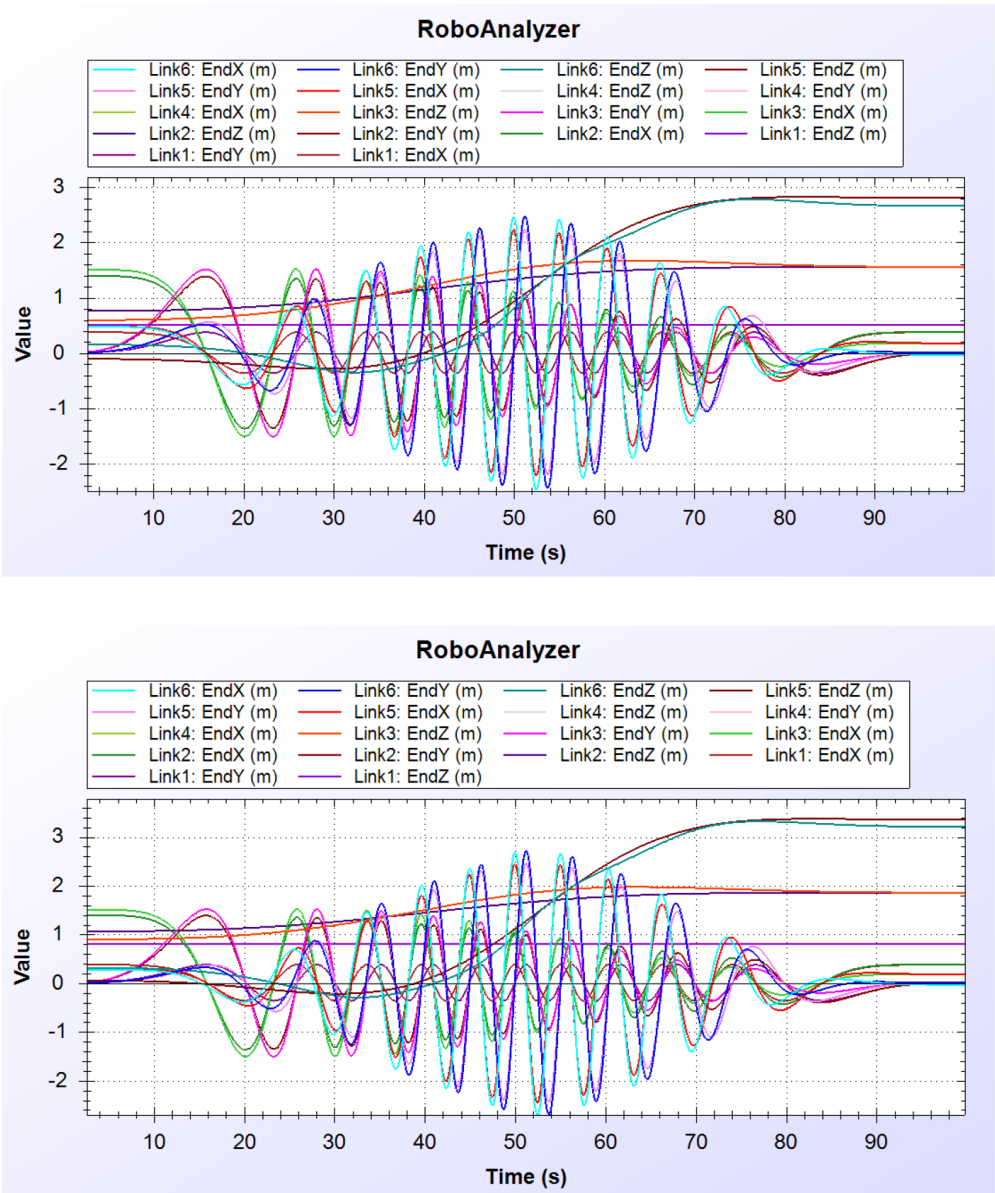

The graphs below (figure 12, 13 & 14) show the velocities, accelerations and forces of all links summarized to make a visual comparison. Whereas it seems for speed and acceleration link 1 plays the main role while for required force link 2 prevails.

FIGURE 12 - Velocities of 6 simulated links

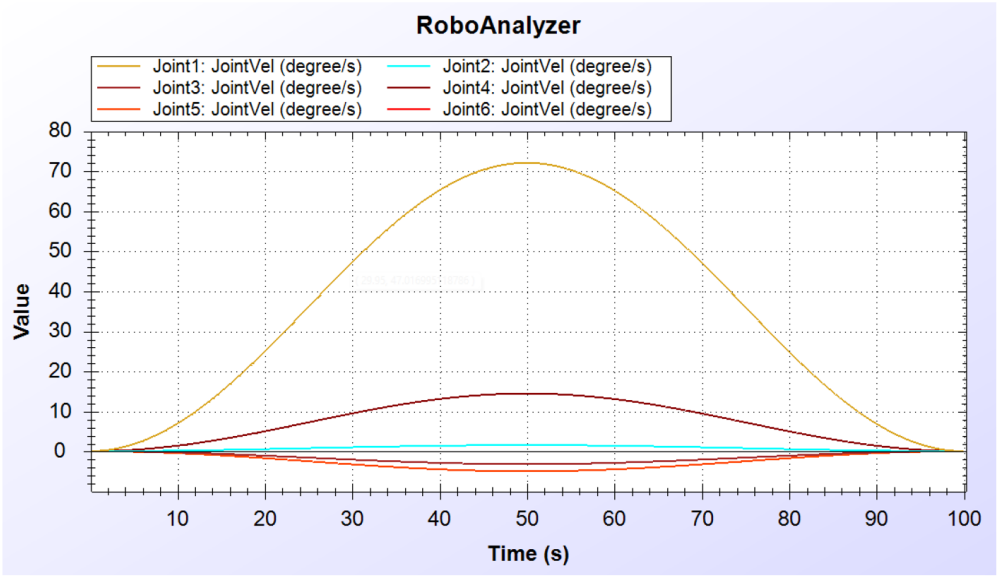

FIGURE 13 - Accelerations of 6 simulated links

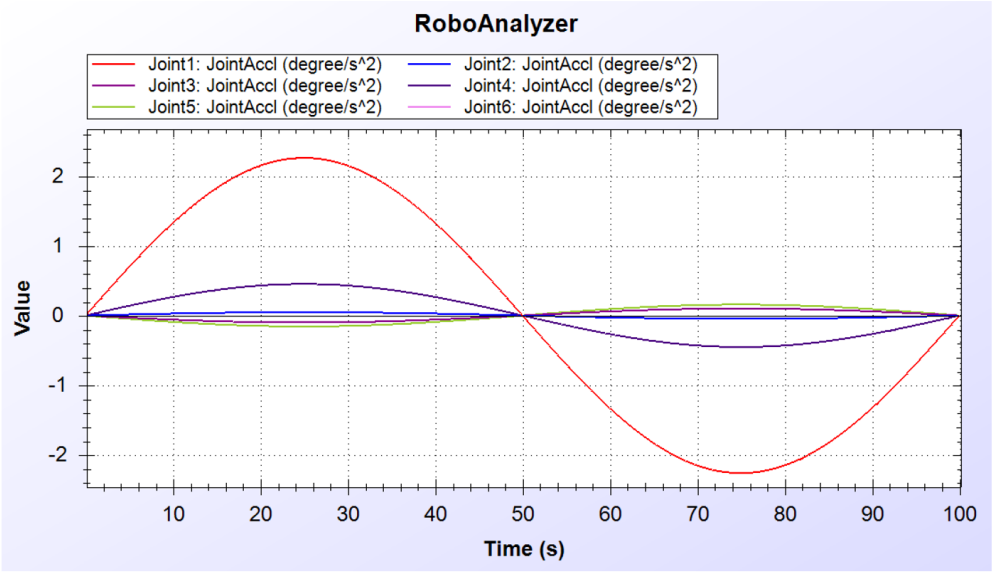

FIGURE 14 - Forces of 6 simulated links before and after modification

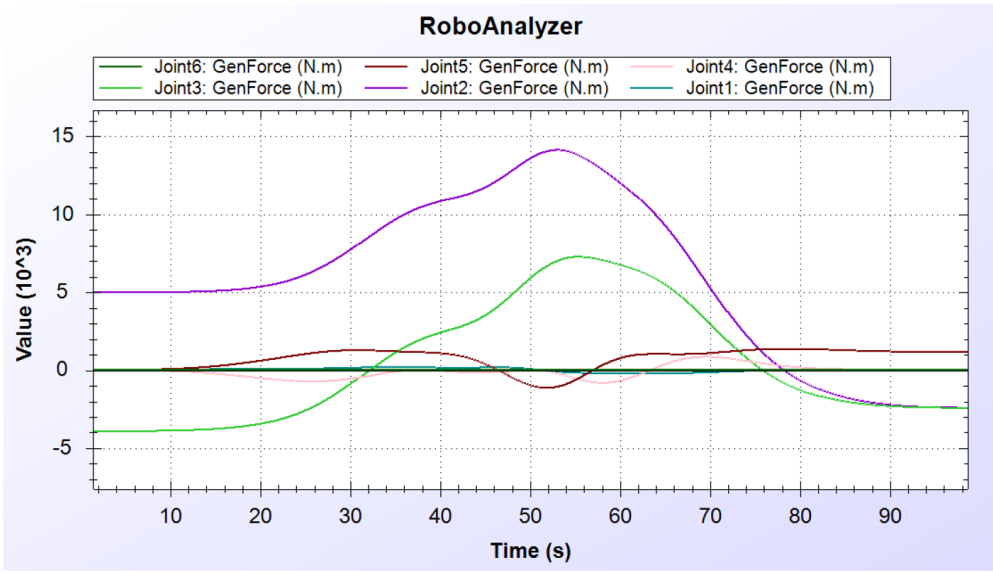

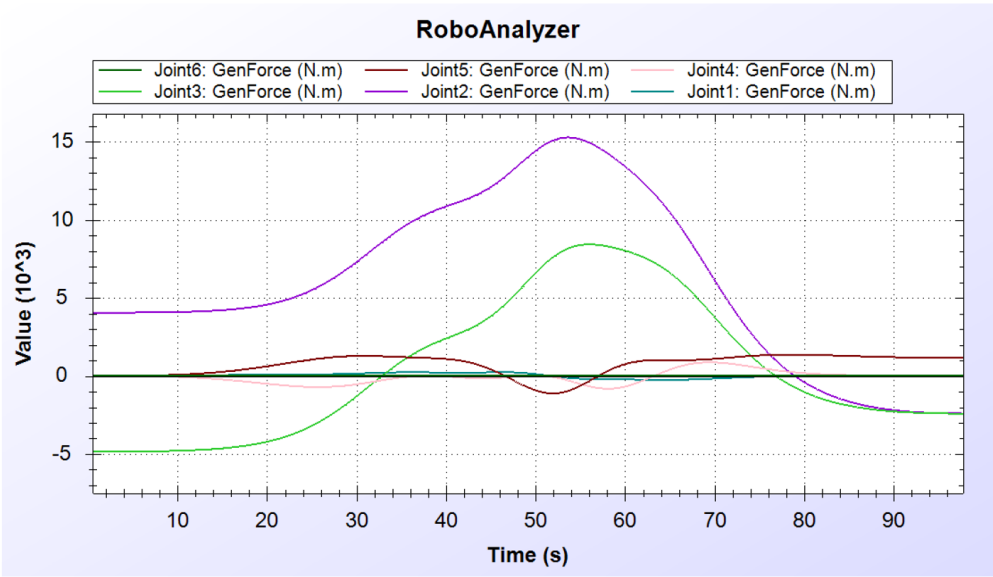

The maximum force that the links can withstand at maximum speed with maximum load, taking into account the inertia, is the total mass of the weight carried by the robot, which is:

360kg + weight of link 6, 20kg + weight of link 5, 20kg + weight of link 4, 60kg + weight of link 3, 240kg + weight of link 2, 280kg = 980kg.

From which the maximum possible moment is calculated 980kg x 9.805m/s2 = 9,609N x 2.56m (arm) = 24,600Nm

This does not account for the weight of the first link as it rotates around the z-axis and does not raise or lower concrete weights even though it carries the total weight of the robot as a quasi-static structure.

The second link has a total moment of 14,110Nm for the manufacturer's structure and 15,252Nm for the proposed structure, these values are far from the 24,600Nm maximum moment of the robot.

This concludes that our modifications of the links are acceptable by the simulation and can withstand the new forces. This leaves the evaluation of the amplifiers and control systems to conclude that these modifications are acceptable in reality without making changes in power and amplification.

4. Electric & electronic configuration

The connection between the components is made according to the scheme in figure 13 where after the voltage input there is protection by means of electrical switches, noise filter and then input to the transformer which makes the conversion to AC 220V and distributes the current to the supply unit (which makes also the conversion to DC 24V), the emergency stop unit and the servo amplifier. Meanwhile, the signals in these components come from the main and secondary panels, which are finally connected to external physical units such as the robot, emergency buttons, controller, ethernet communication, etc.

FIGURE 15 - Connection diagram of the main components

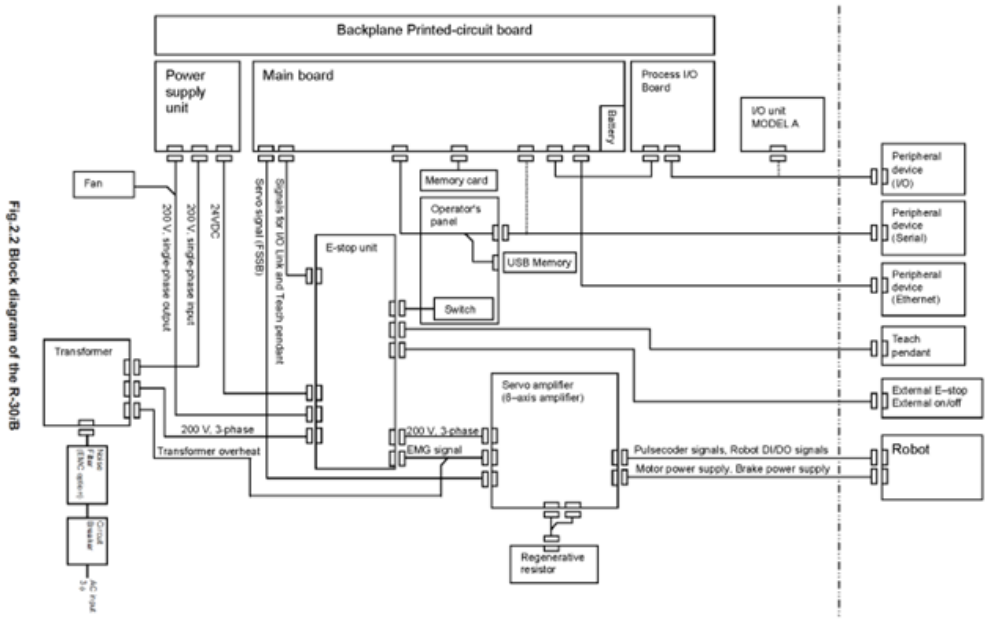

Fig.2.2 Block diagram of the R-30iB

The main board

The main board contains a microprocessor, its peripheral circuits, memory and operator panel control circuitry. The main CPU controls the positioning of the servo mechanism.

- I/O printed circuit board, FANUC MODEL-A I/O unit

Various types of printed circuit boards are available for applications including I/O processing board. FANUC MODEL-A input/output unit can also be installed. When used, different I/O types can be selected. These are connected to the FANUC I/O Link.

- E-stop unit

This unit controls the emergency stop system of the robot controller. It also has the user interface terminal terminals for, relevant safety signals, external on/off signals etc.

- Power supply unit

The power supply unit converts AC power to various levels of DC power.

- Backplane printed circuit

The various control printed circuit boards are mounted on the backplane printed circuit board.

- Controller

All operations including robot programming are performed with this unit. Controller status and data are shown on the liquid crystal display (LCD) on the pendant.

This is also where the peripheral components are connected as in the figure above.

- 6 axis servo amplifier

The servo amplifier controls the servo motor, encoder signal, brake control, travel limits.

- Operator panel

Buttons and LEDs on the operator panel are used to turn on the robot and indicate the status of the robot.

- Transformer

The supply voltage is converted to the required AC voltage for the controller (220V), by the transformer.

- Fan unit, heat exchanger

These components cool the inside of the controller.

- Circuit breaker

If the electrical system in the controller malfunctions, or if the abnormal input power causes high current in the system, the input power is connected to the circuit breaker (switch/circuit breaker) to protect the equipment.

- Regenerative resistance

To discharge the resistive electromotive force from the servo motor, a regenerative resistor is connected to the servo amplifier.

4.1 Servo Amplifier

The servo amplifier is the unit that amplifies the output power that serves to drive the servo motors. As described in the previous chapter, the servo amplifier is supplied with 3-phase current from the emergency stop unit, also at the input are the emergency signals from this unit, the overheating signal from the transformer as well as the command input signals from the main circuit. at the output it is connected to the robot which supplies it with energy and exchanges input-output signals for the movements performed.

FIGURE 16 - Schematic of the power supply for the servo-amplifier

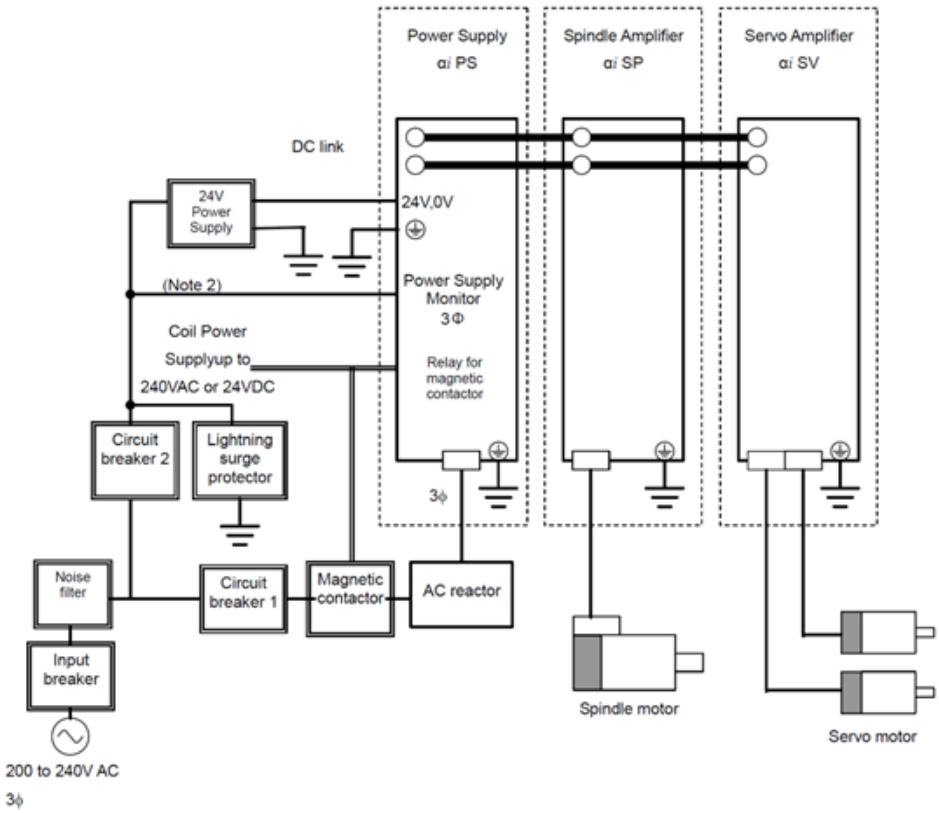

4.2 Servo Motor

The internal circuit of the motor connection is as below (figure 14), where the power comes from the servo amplifier and by means of the pulse coder, the motor returns the signal to the amplifier to make the necessary speed adjustments. Meanwhile, the fan is also connected to the motor, which serves for cooling, grounding for discharging currents, as well as the brakes with DC 24V connection.

FIGURE 17 - Wiring diagram of the servo motor

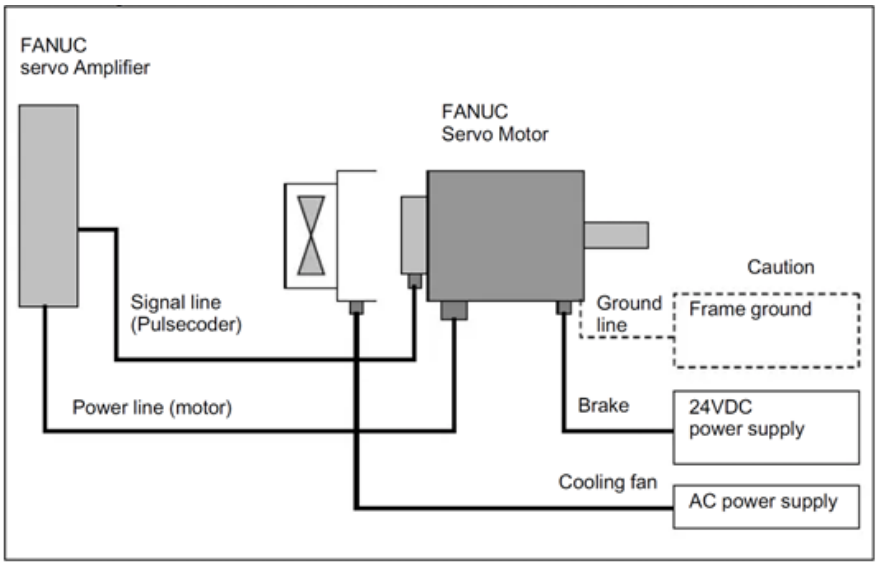

In figure 16 we see the characteristics of the work according to the torque and in overload. The smallest model of this robot is taken as an example to create a general idea of the characteristics of these servo motors.

FIGURE 18 - Operating characteristics of the servo motor

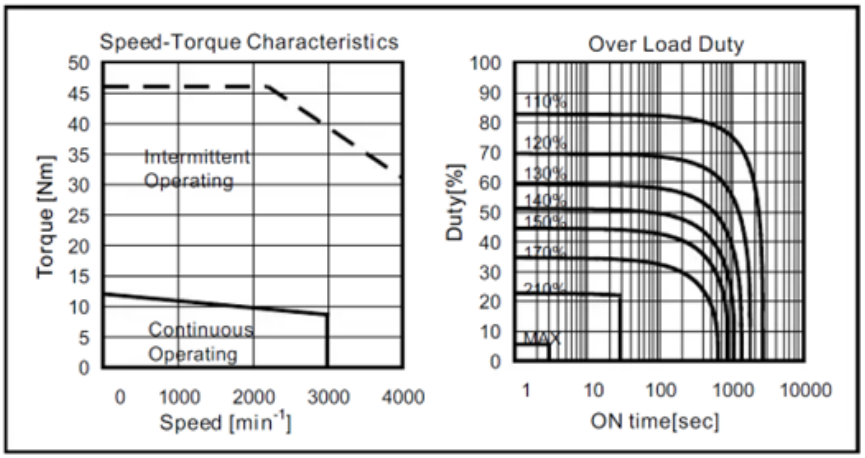

As can be understood from the graph, the maximum speed that the engine reaches in continuous operation is 3000 rpm, while in intermittent operation, but with a higher torque, it exceeds this rotation speed.

In the work with 110% overload, we see the maximum working interval is up to 3000s or 50min and the more the load increases the more the working time decreases and when 200% of the maximum load is reached the engine works only a few seconds before it burns out or fail.

4.3 Response control

In servo motor control, position, speed and torque (torque) are controlled by linking them together. Figure 17 shows a general engine control setup. Servo control is accomplished with this triple block diagram, which has a stream of successive speed changes needed to operate the arbitrary motion, speed command to do position control, torque command to do speed control as well as the subsequent changes in current required to operate at that torque to make current control.

FIGURE 19 - General scheme of control of a servomotor

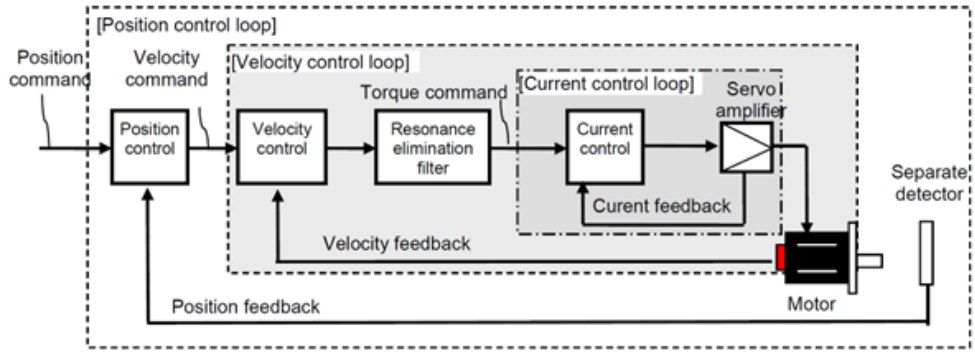

In short, the motor is controlled through individual control of position, speed and current.

In order to increase the tracking performance for position commands and to reduce the contour error, it is necessary to improve the response speed of the speed control and current control. Since each control loop is affected by the internal control loop, servo tuning must be done for the current control loop, speed control loop, and position control loop in the order mentioned in the Figure 17.

Figure 18 shows the resonances created by speed adjustments which are eliminated by the filters explained below.

FIGURE 20 - Schematic of filter resonance adjustment

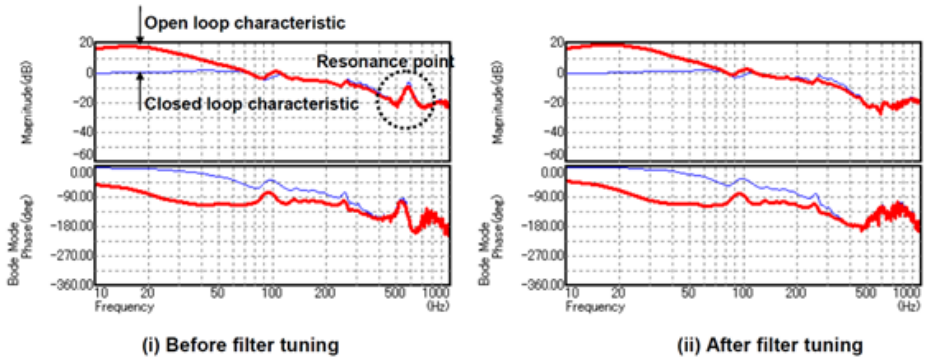

The Resonance Elimination Filter function eliminates vibrations by applying a filter designed to eliminate components from a feedforward command/speed command.

FIGURE 21 - Resonance adjustment filter effects

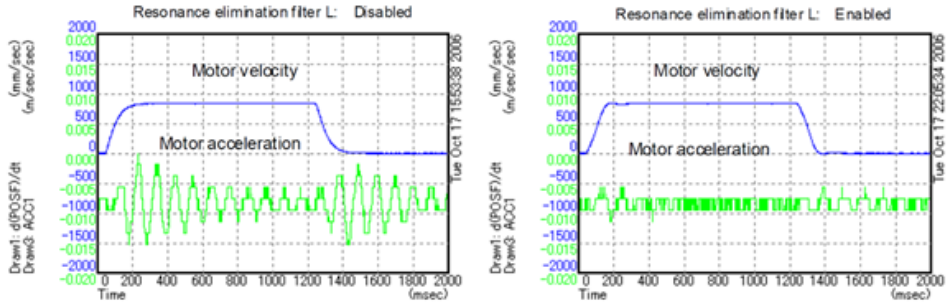

Conclusions

the study and analysis of the dynamics and control of the industrial robot with 6 degrees of freedom FANUC M-900iB/360 brought some valuable conclusions in the engineering nature that help us determine the functionality, capacities and limits of the use and manipulation of this robot.

Mechanical study:
In the mechanical aspect, the physical components of the robot were studied such as the base, links, joints, and end effector, as well as the second part of mechanics which covers topics such as forward kinematics in mathematical form, inverse kinematics and simulated dynamics of the robot.

Mechanical improvements:
Mechanical modification of links 1 and 3 by lengthening them respectively by 0.3m and 0.25m thus increasing the range of the robot's working frame without compromising the electrical and electronic integrity of the system, supported by computer simulations.

FIGURE 22 – AI made final scenario of modified robot between production lines

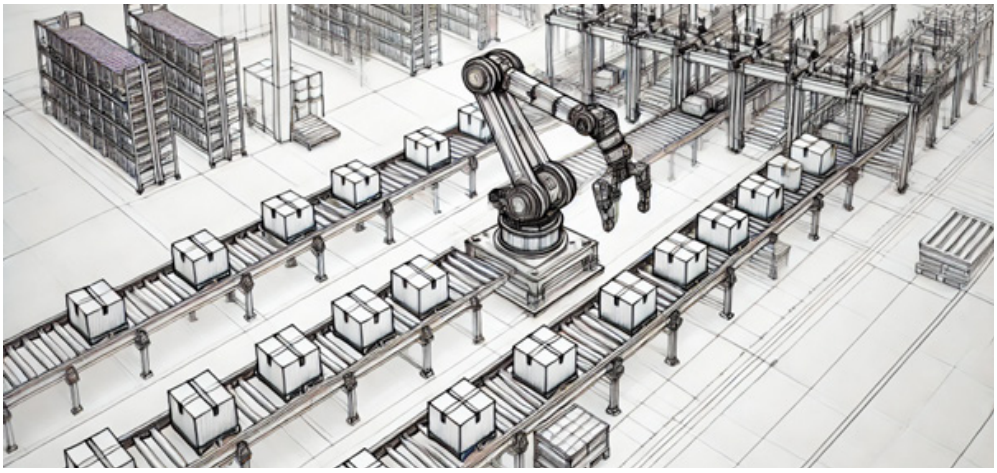

Electrical/electronic study:
In the electrical/electronic aspect, the configuration has been studied in detail to understand how the constituent components are, how they are connected to each other and what functions they have, while in the electronic control method, the general control block-schemas as well as the specific control block-schemas are presented of position, speed and current.

Electrical/Electronic Upgrades:
In the case of upgrading the system and increasing the processing capacity, the same electrical schemes will be used but with improved components such as amplifiers with higher capacity and more powerful servo motors in cases where a radical modification of the system is needed to perform the additional or heavier tasks.

Literature

1. Bilancia, P.& Schmidt, J.& Raffaeli, R.& Peruzzini, M.& Pellicciari, M. (2023). An Overview of Industrial Robots Control and Programming Approaches. Applied Sciences. 13(4):2582.

2. FANUC Robot Series. (2016). R-30iB Controller: Maintenance Manual (8th ed.). FANUC CORPORATION
3. FANUC Robot Series. (2017). R-30iB Controller: Profinet I/O Operator's Manual (4th ed.). FANUC CORPORATION
4. FANUC Robot Series. (2014). R-30iB Controller: KAREL Reference Manual (1st ed.). FANUC CORPORATION
5. FANUC Robot Series. (2016). M-900iB: Mechanical Unit Maintenance Manual (2nd ed.). FANUC CORPORATION
6. FANUC Publications. (2016). Servo Amplifier αi-B Series: Descriptions (2nd ed.). FANUC CORPORATION
7. FANUC Publications. (2015). Servo AC Servo Motor αi-B/ αi Series: Parameter Manual (9th ed.). FANUC CORPORATION
8. FANUC Publications. (2005). Servo AC Servo Motor αis/αi Series: Servo Tuning Procedure. (1st ed.). FANUC CORPORATION
9. Institute of Electrical and Electronics Engineers. Collaborative Control with Industrial Robots; Institute of Electrical and Electronics Engineers: Piscataway, NJ, USA, 2017; ISBN 9781538618837.
10. Lai, R.& Lin, W & Y. Wu, Y. (2018). Review of Research on the Key Technologies Application Fields and Development Trends of Intelligent Robots", International Conference on Intelligent Robotics and Applications, 2018.
11. Tantawi, K.H. & Sokolov, A.& and Tantawi, O. (2019). Advances in Industrial Robotics: From Industry 3.0 Automation to Industry 4.0 Collaboration. 4th Technology Innovation Management and Engineering Science International Conference (TIMES-iCON), Bangkok, Thailand, 2019, pp. 1-4, DOI: 10.1109/TIMES-iCON47539.2019.9024658.